https://doi.org/10.15407/ujpe67.10.722

T. LISSANU,[1] G. KAHSAY,[2] T. NEGUSSIE[2]

[1] Department of Physics, College of Science, Injibara University
(Injibara, P.O Box 40, Ethiopia)
[2] Department of Physics, College of Science, Bahir Dar University
(Bahir Dar, P.O Box 79, Ethiopia)

THEORETICAL INVESTIGATION OF THE SUPERCONDUCTING AND THERMODYNAMIC PROPERTIES OF TWO-BAND MODEL HIGH-TEMPERATURE IRON-BASED SUPERCONDUCTOR $Ba_{1-x}Na_xFe_2As_2$

This work presents the theoretical investigation of the superconducting and thermodynamic properties of the two-band model high-temperature iron-based superconductor $Ba_{1-x}Na_xFe_2As_2$. By developing a model Hamiltonian and by employing the well-known double-time temperature-dependent Green's function formalism, we have computed the superconducting order parameters for the electron and hole intra- and inter-band transitions, superconducting transition temperature, densities of states, and condensation energies. Furthermore, the electronic specific heat and the entropy for electron and hole intra-band transitions have been determined. By using appropriate experimental data and some credible approximations of the parameters in the computed expressions, we have found the phase diagrams of superconducting order parameters versus the temperature, superconducting critical temperature versus the inter-band interaction potential, temperature dependences of the electronic specific heat and entropy for electron and hole intra-band transitions, and densities of states for the electron and hole intra-band transitions as functions of the excitation energy at different values of the temperature. Finally, the phase diagrams of the condensation energy versus the temperature, inter-band pairing potential at $T = 0$ K versus the condensation energy, and condensation energy versus the superconducting transition temperature (T_C) have been drawn. In some of the phase diagrams, the comparison between theoretical and experimental values has been made. The results are in a good agreement with previous findings.

Keywords: order parameters, specific heat, density of states, condensation energy, $Ba_{1-x}Na_xFe_2As_2$.

1. Introduction

The iron-based superconductors are the newly discovered category of superconductors which are becoming promising candidates for the future applications of high-temperature superconductors. The first iron-based superconductor was discovered in 2006 by the research group which found the superconductivity with a transition temperature of about 6 K in LaFePO [1]. This discovery had marked the beginning of a new era in the search for high-temperature iron-based superconductors. Furthermore, the recent discovery of the superconductivity in LaFeAs(O, F) after the replacing phosphorus with arsenic and the doping of the structure by substituting some oxygen atoms with fluorine showed the increase in the tran-

sition temperature up to 26 K [2]. This high T_C has significantly enhanced research activities in the field of IBSCs, particularly when it was found that T_C could be increased up to 43 K by applying pressure [3]. In IBSCs such as $RFeAsO_{1-x}F$ (where, R = La, Sm, Ce, Nd, Pr, Gd), with considerably high critical temperature of up to 56 K, the superconductivity occurs in the FeAs layers and the LaO layers are supposed to be charged reservoirs when doped with F ions. In addition, multiband iron-based superconductors were discovered, and the superconductivity in the 122-family with $T_C = 38$ K in hole-doped superconductor $Ba_{0.6}K_{0.4}Fe_2As_2$ was observed [4].

As is well known, IBSCs have high superconducting transition temperature, large upper critical magnetic field, high critical current density, and relatively low anisotropy which are the fundamental requirements for large current and (or) high magnetic field applications of superconductors. An important feature of the iron-based pnictides is their multiband electronic structures with both electron and hole bands at the Fermi level [5]. These have key features of such inter-band pairing mechanisms that can generate or enhance superconducting pairing irrespective of whether it is attractive or repulsive [6]. The pairing mechanism in the iron-based pnictides is extensively considered to be mediated by spin fluctuations [7]. Amongst the high-temperature iron-based pnictides, the 122-family compounds such as the (AE, K) Fe_2As_2 (where, AE = Ba, Sr) have been considered as promising superconducting materials for upcoming applications, since a high critical current density is believed to exist in the superconducting wires and tapes [8]. $Ba_{0.6}Na_{0.4}Fe_2As_2$ optimally Na-doped with a concentration of $x = 0.4$ has a superconducting transition temperature of about 34 K [9]. The hole doping does remove charge carriers to the system or FeAs layer, and the dopant changes the electronic structure. The Fermi surface of hole-doped $Ba_{1-x}Na_xFe_2As_2$ is, to a large extent, the same as the Fermi surface found for the K-doped compounds suggesting a similar impact on the substitution of Ba by either K or Na on the electronic band dispersion at the Fermi level [9].

The multiple gap structures in the 122 system have clear evidences and are provided by specific heat and angle-resolved photoemission spectroscopy measurements [10, 11]. Numerous intra-bands and inter-band interaction terms exist in the multiband model of iron-based superconductivity. The inter-band pairing is important in multiband models [12]. The optimally hole-doped $Ba_{1-x}Na_xFe_2As_2$ with $x = 0.35$ iron-based pnictides of the Fermi surface comprises of multiple Fermi surface sheets. ARPES studies in the 122- family revealed the presence of hole-like and electron-like Fermi surfaces at the center of the Brillouin zone and at the corner, respectively, and the cylindrical shape of the electron-like Fermi surfaces at the zone corner are usually attributed to the electronic structure in high-T_C 122-family superconductors. All the 5Fe (3d) orbitals pass via the Fermi surfaces in the 122-family of the IBSCs. The first principal computations have demonstrated that the energy bands near the Fermi surface are attributed mainly to the Fe (3d) orbitals [13], and the states with energy at the Fermi level are formed by the 3d electrons of Fe, and the superconductivity is mainly due to these 3d states, as is shown by the density functional calculations [14].

The hole-doped two-band $Ba_{1-x}Na_xFe_2As_2$ (with $x = 0.35$) IBSC has two superconducting order parameters for electron and hole intra-band transitions for electron and hole bands, respectively. Both vanish at the same superconducting transition temperature (T_C) of $Ba_{1-x}Na_xFe_2As_2$. The electron and hole intra-bands have their own coupling pairing potentials of electron and hole intra-band transitions, respectively, and the inter-band pairing interaction potentials. The existence of inter-band pairing interaction potential improves the pairing of the electrons and leads to the vanishing of electron and hole intra-band transitions at the same superconducting transition temperature, even though they are different at zero temperature [15]. At the zero temperature, the experimental values of superconducting energy gaps for $Ba_{1-x}Na_xFe_2As_2$ on the electron Fermi surface and on the hole Fermi surface are 8.5 meV and 3.6 meV, respectively [16].

2. Materials and Methods

The mathematical formulation of the Hamiltonian of the system in the two-band model high-temperature IBSC $Ba_{1-x}Na_xFe_2As_2$ which consists of the electron and hole intra-band and inter-band terms is expressed as [17–19],

$$\hat{H} = \hat{H}_e + \hat{H}_h + \hat{H}_{eh}, \tag{1}$$

where

$$\hat{H}_e = \sum_{k\sigma} \varepsilon_e(k)\hat{C}^+_{k\sigma}\hat{C}_{k\sigma} - \\ - \sum_{k,k'} U_e(k,k')\hat{C}_{k\uparrow}\hat{C}^+_{-k\downarrow}\hat{C}_{-k'\downarrow}\hat{C}_{k'\uparrow}, \quad (2)$$

$$\hat{H}_h = \sum_{k\sigma} \varepsilon_h(k)\hat{d}^+_{k\sigma}\hat{d}_{k\sigma} - \\ - \sum_{k,k'} U_h(k,k')\hat{d}^+_{k\uparrow}\hat{d}^+_{-k\downarrow}\hat{d}_{-k'\downarrow}\hat{d}_{k'\uparrow}, \quad (3)$$

$$\hat{H}_{eh} = -\sum_{k.k'} U_{eh}(k,k') \times \\ \times \left[\hat{C}^+_{k\uparrow}C^+_{-k\downarrow}\hat{d}_{-k'\downarrow}\hat{d}_{k'\uparrow} + \hat{d}^+_{k\uparrow}\hat{d}^+_{-k\downarrow}\hat{C}_{-k'\downarrow}\hat{C}_{k'\uparrow}\right]. \quad (4)$$

Now, using (2)–(4) in (1), we obtain

$$\hat{H} = \sum_{k,\sigma} \varepsilon_e(k)\hat{C}^+_{k\sigma}\hat{C}_{k\sigma} + \sum_{k,\sigma} \varepsilon_h(k)\hat{d}^{+=}_{k\sigma}\hat{d}_{k\sigma} - \\ - \sum_{k,k'} U_e(k,k')(\hat{C}^+_{k\uparrow}\hat{C}^+_{-k\downarrow}\langle\hat{C}_{-k'\downarrow},\hat{C}_{k'\uparrow}\rangle + \\ + \langle\hat{C}^+_{k\uparrow},C^+_{-k\downarrow}\rangle\hat{C}_{-k'\downarrow}\hat{C}_{k'\uparrow}\rangle) - \\ - \sum_{k,k'} U_h(k,k')(\hat{d}^+_{k\uparrow}\hat{d}^+_{-k\downarrow}\langle\hat{d}_{-k'\downarrow}\hat{d}_{k'\uparrow}\rangle + \\ + \langle\hat{d}^+_{k\uparrow}\hat{d}^+_{-k\downarrow}\rangle\hat{d}_{-k'\downarrow}\hat{d}_{k\uparrow}) - \sum_{k,k'} U_{eh}(k,k') \times \\ \times (\hat{C}^+_{k\uparrow}\hat{C}^+_{-k\downarrow}\langle\hat{d}_{-k'\downarrow}\hat{d}_{k'\uparrow}\rangle + \langle\hat{C}^+_{K\uparrow}\hat{C}^+_{-k\downarrow}\rangle\hat{d}_{-k'\uparrow}\hat{d}_{k'\uparrow}) - \\ - \sum_{k,k'} U_{eh}(k,k')(\hat{d}^+_{k\uparrow}\hat{d}^+_{-k\downarrow}\langle\hat{C}_{-k'\downarrow}\hat{C}_{k'\uparrow}\rangle + \\ + \langle\hat{d}^+_{k\uparrow}\hat{d}^+_{-k\downarrow}\rangle\hat{C}_{-k'\downarrow}\hat{C}_{k'\uparrow}). \quad (5)$$

For

$$\Delta_e = \sum_{k,k'} U_e(k,k')\langle\hat{C}_{-k'\downarrow}\hat{C}_{k'\uparrow}\rangle = \\ = \sum_{k,k'} U_e(k,k')\langle\hat{C}^+_{k\uparrow},\hat{C}^+_{-k\downarrow}\rangle, \quad (6)$$

$$\Delta_h = \sum_{k,k'} U_h(k,k')\langle\hat{d}_{-k'\downarrow}\hat{d}_{k'\uparrow}\rangle = \\ = \sum_{k,k'} U_h(k,k')\langle\hat{d}^+_{k\uparrow},\hat{d}^+_{-k\downarrow}\rangle. \quad (7)$$

and

$$\Delta_{eh} = \sum_{k,k'} U_{eh}(k,k')\langle\hat{C}_{-k'\downarrow}\hat{C}_{k'\uparrow}\rangle = \\ = \sum_{k,k'} U_{eh}(k,k')\langle\hat{d}^{'}_{-k'\uparrow}\hat{d}_{k'\uparrow}\rangle,$$

$$\Delta_{eh} = \sum_{k,k'} U_e(k,k')\langle\hat{C}^+_{k\uparrow},\hat{C}^+_{-k\downarrow}\rangle = \\ = \sum_{k,k'} U_{eh}(k,k')\langle\hat{d}^+_{k\uparrow},\hat{d}^+_{-k\downarrow}\rangle, \quad (8)$$

we get

$$\hat{H} = \sum_{k,\sigma} \varepsilon_e(k)\hat{C}^+_{k\sigma}\hat{C}_{k\sigma} + \sum_{k,\sigma} \varepsilon_h(k)\hat{d}^+_{k\sigma}\hat{d}_{k\sigma} - \\ - \Delta_e \sum_{k,k'} (\hat{C}^+_{k\uparrow}\hat{C}^+_{-k\uparrow} + \hat{C}_{-k'\downarrow}\hat{C}_{k'\uparrow}) - \\ - \Delta_h \sum_{k,k'} (\hat{d}^+_{k\uparrow}\hat{d}^+_{-k\downarrow} + \hat{d}_{-k'\downarrow}\hat{d}_{k\uparrow}) - \\ - \Delta_h \sum_{k,k'} (\hat{d}^+_{k\uparrow}\hat{d}^+_{-k\downarrow} + \hat{d}_{-k\downarrow}\hat{d}_{k'\uparrow}) - \\ - \Delta_{eh} \sum_{k,k'} (\hat{C}^+_{k\uparrow}\hat{C}^+_{-k\downarrow} + \hat{d}_{-k'\downarrow}\hat{d}_{k'\uparrow}) - \\ - \Delta_{eh} \sum_{k,k'} (\hat{d}^+_{k\uparrow}\hat{d}^+_{-k\downarrow} + \hat{C}_{-k'\downarrow}\hat{C}_{k'\uparrow}), \quad (9)$$

where, the first two terms are the energy of conduction electrons and holes, respectively, the next two terms involve the superconductivity due to the intraparing at the electron and hole Fermi surfaces, respectively. The last two terms represent the superconductivity due to the inter-band transitions between the two bands. $\hat{C}^+_{k\uparrow}(\hat{C}_{-k\downarrow})$ and $\hat{d}^+_{k\uparrow}(\hat{d}_{-k\downarrow})$ are the creation (annihilation) operators in the electron and the hole bands, respectively.

2.1. Electron and hole intra-band and inter-band dependences on the temperature

By using the double-time temperature-dependent Green's function formalism, the equation of motion for the superconducting correlation function $\langle\langle\hat{C}^+_{k\uparrow},\hat{C}^+_{-k\downarrow}\rangle\rangle$ in the electron intra-band is expressed as [20]

$$\omega\langle\langle\hat{C}^+_{k\uparrow},\hat{C}^+_{-k\downarrow}\rangle\rangle = \langle\langle[\hat{C}^+_{k\uparrow},\hat{C}^+_{-k\downarrow}] + \langle\langle[\hat{C}^+_{k\uparrow},\hat{H}],\hat{C}^+_{-k\downarrow}\rangle\rangle, \\ \omega\langle\langle\hat{C}^+_{k\uparrow},\hat{C}^+_{-k\downarrow}\rangle\rangle = \langle\langle[\hat{C}^+_{k\uparrow},\hat{H}_e + \hat{H}_h + \hat{H}_{eh}],\hat{C}^+_{-k\downarrow}\rangle\rangle. \quad (10)$$

Now, performing the commutation relation for $\left[\hat{C}^{+}_{k\uparrow}, \hat{H}_e\right]$, we get

$$\left[\hat{C}^{+}_{k\uparrow}, \hat{H}_e\right] = \left[\hat{C}^{+}_{k\uparrow,} \sum_{k,\sigma} \varepsilon_e(k)\hat{C}^{+}_{k\sigma}\hat{C}_{k\sigma} - \right.$$
$$\left. - \Delta_e \sum_{k,k'} (\hat{C}^{+}_{k\uparrow}\hat{C}^{+}_{-k\downarrow} + \hat{C}_{-k'\downarrow}\hat{C}_{k'\uparrow}\rangle\right].$$

Using the commutation and anticommutation rules, we obtain

$$\left[\hat{C}^{+}_{k\uparrow}, \hat{H}_e\right] = -\varepsilon_e \hat{C}^{+}_{k\uparrow} + \Delta_e \hat{C}_{-k'\downarrow}. \tag{11}$$

Similarly, the commutation relation for $\left[\hat{C}^{+}_{k\uparrow}, \hat{H}_h\right]$ yields

$$\left[\hat{C}^{+}_{k\uparrow}, \hat{H}_h\right] = \left[\hat{C}^{+}_{k\uparrow,} \sum_{k,\sigma} \varepsilon_h(k)\hat{d}^{+}_{k\sigma}\hat{d}_{k\sigma} - \right.$$
$$\left. - \Delta_h \sum_{k,k'} (\hat{d}^{+}_{k\uparrow}\hat{d}^{+}_{-k\downarrow} + \hat{d}_{-k'\downarrow}\hat{d}_{k'\uparrow}\rangle\right].$$

From this expression, we get

$$\left[\hat{C}^{+}_{k\uparrow}, \hat{H}_h\right] = 0. \tag{12}$$

Furthermore, the commutation relation for $\left[\hat{C}^{+}_{k\uparrow}, \hat{H}_{eh}\right]$ is given by

$$\left[\hat{C}^{+}_{k\downarrow}, \hat{H}_{eh}\right] = \left[\hat{C}^{+}_{k\uparrow}, -\Delta_{eh} \sum_{k,k'} (\hat{C}^{+}_{k\uparrow}\hat{C}^{+}_{-k\downarrow} + \hat{d}_{-k'\downarrow}\hat{d}_{k'\uparrow}) - \right.$$
$$\left. - \Delta_{eh} \sum_{k,k'} (\hat{d}^{+}_{k\uparrow}\hat{d}^{+}_{-k\downarrow} + \hat{C}_{-k'\downarrow}\hat{C}_{k'\uparrow})\right],$$
$$\left[\hat{C}^{+}_{k\uparrow}, \hat{H}_{eh}\right] = -\Delta_{eh} \sum_{k,k'} \left(\left[\hat{C}^{+}_{k\uparrow}, \hat{C}^{+}_{k\uparrow}\right] + \right.$$
$$\left. + \left[(\hat{C}^{+}_{k\uparrow}, \hat{d}_{-k'\downarrow}\hat{d}_{k'\uparrow}\right]\right) -$$
$$- \Delta_{eh} \sum_{k,k'} \left(\left[\hat{C}^{+}_{k\uparrow}, \hat{d}^{+}_{k\uparrow}\hat{d}^{+}_{-k\downarrow}\right] + \left[\hat{C}^{+}_{k\uparrow}, \hat{C}_{-k'\downarrow}\hat{C}_{k'\uparrow}\right]\right).$$

Hence we get

$$\left[\hat{C}^{+}_{k\uparrow}, \hat{H}_{eh}\right] = \Delta_{eh}\hat{C}_{-k'\downarrow}. \tag{13}$$

Using (11)–(13) in (10) the equation of motion for the superconducting correlation function $\langle\langle \hat{C}^{+}_{k\uparrow}, \hat{C}^{+}_{-k\downarrow}\rangle\rangle$, becomes,

$$\omega\langle\langle \hat{C}^{+}_{k\uparrow}, \hat{C}^{+}_{-k\downarrow}\rangle\rangle = -\varepsilon_e\langle\langle \hat{C}^{+}_{k\uparrow}, \hat{C}^{+}_{-k\downarrow}\rangle\rangle +$$
$$+ \Delta_e\langle\langle \hat{C}_{-k'\downarrow}, \hat{C}^{+}_{-k\downarrow}\rangle\rangle + \Delta_{eh}\langle\langle \hat{C}_{-k'\downarrow}, \hat{C}^{+}_{-k\downarrow}\rangle\rangle.$$

Thus, the expression for the equation of motion becomes

$$\langle\langle \hat{C}^{+}_{k\uparrow,}\hat{C}^{+}_{-k\downarrow}\rangle\rangle = \frac{\Delta_e + \Delta_{eh}}{\omega + \varepsilon_e(k)} \langle\langle \hat{C}_{-k'\downarrow}, \hat{C}^{+}_{-k\downarrow}\rangle\rangle. \tag{14}$$

Similarly, the equation of motion for $\langle\langle \hat{C}_{-k'\downarrow}, \hat{C}^{+}_{-k\downarrow}\rangle\rangle$ is given by

$$\begin{aligned}
&\omega\langle\langle \hat{C}_{-k'\downarrow}, \hat{C}^{+}_{-k\downarrow}\rangle\rangle = \langle[\hat{C}_{-k'\downarrow}, C^{+}_{-k\downarrow}]\rangle + \\
&+ \langle\langle[\hat{C}_{-k'\downarrow}, \hat{H}], \hat{C}^{+}_{-k\downarrow}\rangle\rangle, \\
&\omega\langle\langle \hat{C}_{-k'\downarrow}, \hat{C}^{+}_{-k\downarrow}\rangle\rangle = 1 + \langle\langle[\hat{C}_{-k'\downarrow}, \hat{H}_e] + \\
&+ [\hat{C}_{-k'\downarrow}, \hat{H}_h] + [\hat{C}_{-k\downarrow}, \hat{H}_{eh}], \hat{C}^{+}_{-k\downarrow}\rangle\rangle.
\end{aligned} \tag{15}$$

Now, evaluating the commutation relations given in (15), we get

$$\left[\hat{C}_{-k'\downarrow}, \hat{H}_e\right] = \left[\hat{C}_{-k'\downarrow}, \sum_{k\sigma} \varepsilon_e(k)\hat{C}^{+}_{k\sigma}\hat{C}_{k\sigma} - \right.$$
$$\left. - \Delta_e \sum_{k,k'} (\hat{C}^{+}_{k\uparrow}\hat{C}^{+}_{-k\downarrow} + \hat{C}_{-k'\downarrow}\hat{C}_{k'\uparrow}\right],$$
$$\left[\hat{C}_{-k'\downarrow}, \hat{H}_e\right] = \sum_{k\sigma} \varepsilon_e(k) \left[\hat{C}_{-k'\downarrow}, \hat{C}^{+}_{K\sigma}\hat{C}_{k\sigma}\right] - \Delta_e \times$$
$$\times \sum_{k,k'} \left[\hat{C}_{-k'\downarrow}, \hat{C}^{+}_{k\uparrow}\hat{C}^{+}_{-k\downarrow}\right] - \Delta_e \sum_{k,k'} \left[\hat{C}_{-k'\downarrow}, \hat{C}_{k'\downarrow}\hat{C}^{+}_{k'\uparrow}\right].$$

Hence, we get

$$\left[\hat{C}_{-k'\downarrow}, \hat{H}_e\right] = \varepsilon_e(k)\hat{C}_{-k'\downarrow} + \Delta_e\hat{C}^{+}_{k\uparrow}. \tag{16}$$

Performing a similar commutation for $\left[\hat{C}_{-k\downarrow}, \hat{H}_h\right]$, as for the electron above, we obtain

$$\left[\hat{C}^{+}_{k\uparrow}, \hat{H}_h\right] = \left[\hat{C}^{+}_{k\uparrow}, \sum_{k,\sigma} \varepsilon_h(k)\hat{d}^{+}_{k\sigma}\hat{d}_{k\sigma} - \right.$$
$$\left. - \Delta_h \sum_{k,k'} (\hat{d}^{+}_{k\uparrow}\hat{d}^{+}_{-k\downarrow} + \hat{d}_{-k'\downarrow}\hat{d}_{k'\uparrow})\right].$$

From which, we get

$$\left[\hat{C}_{-k'\downarrow}, \hat{H}_h\right] = 0. \tag{17}$$

Similarly, the commutation relation for $\left[\hat{C}_{-k'\downarrow}, \hat{H}_{eh}\right]$ yields

$$\left[\hat{C}_{-k'\downarrow}, \hat{H}_{eh}\right] =$$

$$= \left[\hat{C}_{-k'\downarrow}, -\Delta_{eh}\sum_{k,k'}\left(\hat{C}^{+}_{k\uparrow}\hat{C}^{+}_{-k\downarrow}, \hat{d}_{-k'\downarrow}\hat{d}_{k'\downarrow}\right)\right] -$$
$$- \left[\hat{C}_{-k'\downarrow}, \Delta_{eh}\sum_{k,k'}\left(\hat{d}^{+}_{k\uparrow}\hat{d}^{+}_{-k\downarrow} + \hat{C}_{-k'\downarrow}\hat{C}_{k'\uparrow}\right)\right].$$

Thus, we get

$$\left[\hat{C}_{-k'\downarrow}, \hat{H}_{eh}\right] = \Delta_{eh}\hat{C}^{+}_{k\uparrow}. \tag{18}$$

Now, using (16)–(18) in (15), the equation of motion for the superconducting correlation function $\langle\langle \hat{C}_{-k'\downarrow}, \hat{C}^{+}_{-k\downarrow}\rangle\rangle$ becomes

$$\omega\langle\langle \hat{C}_{-k'\downarrow}, \hat{C}^{+}_{-k\downarrow}\rangle\rangle = 1 + \langle\langle \varepsilon_e(k)\hat{C}_{-k'\downarrow} +$$
$$+ \Delta_e\hat{C}^{+}_{k\uparrow} + \Delta_{eh}C^{+}_{k\uparrow}\hat{C}^{+}_{-k\downarrow}\rangle\rangle.$$

Hence, we get

$$\langle\langle \hat{C}_{-k'\downarrow}, \hat{C}^{+}_{-k\downarrow}\rangle\rangle = \frac{1}{\omega - \varepsilon_e(k)} +$$
$$+ \frac{\Delta_e + \Delta_{eh}}{\omega - \varepsilon_e(k)}\langle\langle C^{+}_{k\uparrow}, \hat{C}^{+}_{-k\downarrow}\rangle\rangle. \tag{19}$$

Substituting (19) into (14) yields

$$\langle\langle \hat{C}_{-k'\downarrow}, \hat{C}^{+}_{-k\downarrow}\rangle\rangle = \frac{\Delta_e + \Delta_{eh}}{\omega + \varepsilon_e(k)}\left(\frac{1}{\omega - \varepsilon_e(k)} +\right.$$
$$\left. + \frac{\Delta_e + \Delta_{eh}}{\omega - \varepsilon_e(k)}\langle\langle C^{+}_{k\uparrow}, \hat{C}^{+}_{-k\downarrow}\rangle\rangle\right).$$

Hence we get

$$\langle\langle \hat{C}_{-k'\downarrow}, \hat{C}^{+}_{-k\downarrow}\rangle\rangle = \frac{\Delta_e + \Delta_{eh}}{\omega^2 - \varepsilon^2_e(k) - (\Delta_e + \Delta_{eh})}. \tag{20}$$

The superconducting order parameter in an electron band can be related to the Green's function as

$$\Delta_e = \frac{U_e}{2\beta}\sum_k \langle\langle \hat{C}^{+}_{k\uparrow}, \hat{C}^{+}_{-k\downarrow}\rangle\rangle, \tag{21}$$

where $\beta = \frac{1}{k_{\mathrm{B}}T}$, k_{B} is the Boltzmann constant, and U_e is the pairing potential in the electron band.

Now, we use the relation $\omega \to i\omega_n$ and Matsubara's frequency [21] given by

$$\omega_n = \frac{(2n+1)\pi}{\beta}. \tag{22}$$

Using (20) and (22) in (21), we obtain

$$\Delta_e = \frac{U_e\beta}{2} \times$$
$$\times \sum_{k,n}\left(\frac{\Delta_e + \Delta_{eh}}{((2n+1)\pi)^2 + \beta^2(\varepsilon^2_e(k) + (\Delta_e + \Delta_{eh})^2)}\right). \tag{23}$$

Introducing the density of states at the Fermi level, changing the summation into integration, and using the relation

$$\sum_{k,n}\frac{1}{((2n+1)\pi)^2 + (\beta E)^2} = \frac{\tanh(\beta E/2)}{2\beta E}, \tag{24}$$

we get

$$\Delta_e = U_e D_e(0)\Delta_e \int_0^{\hbar\omega_{\mathrm{F}}} \frac{\tanh\left(\frac{\beta E_e(k)}{2}\right)}{E_e(k)}\, dE_e(k) +$$
$$+ U_{eh}D_h(0)\Delta_h \int_0^{\hbar\omega_{\mathrm{F}}} \frac{\tanh\left(\frac{\beta E_h(k)}{2}\right)}{E_h(k)}\, dE_h(k), \tag{25}$$

where $E^2_e(k) = \varepsilon^3_e(k) + (\Delta_e + \Delta_{eh})^2$ and

$E^2_h(k) = \varepsilon^3_h(k) + (\Delta_h + \Delta_{eh})^2$.

Now, if we consider the electron intra-band transition only, (25) becomes

$$\frac{1}{U_e N_e(0)} = \int_0^{\hbar\omega_{\mathrm{F}}} \frac{\tanh\left(\frac{\beta(\varepsilon^2_e(k) + \Delta^2_e)^{\frac{1}{2}}}{2}\right)}{(\varepsilon^2_e(k) + \Delta^2_e)^{\frac{1}{2}}}\, d\varepsilon_e(k). \tag{26}$$

By using the Laplace transformation, the integral in (26) yields

$$\frac{1}{U_e N_e(0)} = \int_0^{\hbar\omega_{\mathrm{F}}} \frac{\tanh\left(\frac{\sqrt{\varepsilon^2_e(k) + \Delta^2_e}}{2}\right)}{\sqrt{\varepsilon^2_e(k) + \Delta^2_e}}\, d\varepsilon_e(k) -$$
$$- 4\beta^2\Delta^2_e \int_0^{\hbar\omega_{\mathrm{F}}} \sum_0 \frac{1}{\pi(2n+1)^4\left(1 + \left(\frac{\beta\varepsilon_e(k)}{\pi(2n+1)}\right)^2\right)^2} \tag{27}$$

Using the integration by parts and substitution methods, (27) reduces to

$$\frac{1}{U_e D_e(0)} = \ln\left(1.14\frac{\hbar\omega_{\mathrm{F}}}{k_{\mathrm{B}}T}\right)\frac{-4\Delta^2_e\beta^2}{\pi^3} \times$$
$$\times \sum_0^{\infty}\frac{1}{(2n+1)^3}\int_0^{\infty}\frac{1}{(1+z^2)^2}dz, \tag{28}$$

where $z = \frac{\beta\varepsilon_e(k)}{\pi(2n+1)}$.

Applying the Zeta and Riemann zeta functions, (28) becomes

$$\frac{1}{U_e D_e(0)} = \ln\left(1.14\frac{\hbar\omega_{\rm F}}{k_{\rm B}T}\right) - \frac{\Delta_e^2}{k_{\rm B}^2T^2}(0.1065). \quad (29)$$

Using [22], (29) becomes

$$\frac{1}{U_e D_e(0)} = \ln\left(1.14\frac{\hbar\omega_{\rm F}}{k_{\rm B}T}\right). \quad (30)$$

Substituting (30) into (29) and using the relation

$$\ln(1-x) = -x - \frac{x^2}{2} + ...,$$

we get

$$\Delta_e = 3.06\, k_{\rm B}T_C\left(1-\frac{T}{T_C}\right)^{\frac{1}{2}}. \quad (31)$$

From the well-known BCS theory [22], we have

$$T_C = 1.14\,\frac{\hbar\omega_{\rm F}}{k_{\rm B}}\exp\left(-\frac{1}{U_e D_e(0)}\right). \quad (32)$$

Now, substituting (32) into (31), the superconducting order parameter in the electron band becomes

$$\Delta_e(T) = 3.49\hbar\omega_{\rm F}\exp\left(-\frac{1}{U_e D_e(0)}\right)\left(1-\frac{T}{T_C}\right)^{\frac{1}{2}}. \quad (33)$$

Following the same procedure as for the electron intra-band traditions, the equation of motion for the superconducting correlation functions $\langle\langle \hat{d}^+_{k\uparrow}, \hat{d}^+_{-k\downarrow}\rangle\rangle$ for the hole intra-band transitions can be computed in the form

$$\langle\langle \hat{d}^+_{k\uparrow}, \hat{d}^+_{-k\downarrow}\rangle\rangle = \frac{\Delta_h + \Delta_{eh}}{\omega + \varepsilon_h(k)}\langle\langle \hat{d}_{-k'\downarrow}, \hat{d}^+_{-k\downarrow}\rangle\rangle. \quad (34)$$

and

$$\langle\langle \hat{d}_{-k'\downarrow}\hat{d}^+_{-k\downarrow}\rangle\rangle = \frac{1}{\omega - \varepsilon_h(k)}\frac{\Delta_h + \Delta_{eh}}{\omega - \varepsilon_h(k)}\,\langle\langle \hat{d}^+_{k\uparrow}, \hat{d}^+_{k\uparrow}\rangle\rangle. \quad (35)$$

After a couple of steps, the expression for the superconducting order parameter in the hole band $\Delta_h(T)$ is given by

$$\Delta_h(T) = 3.49\,\hbar\,\omega_{\rm F}\exp\left(-\frac{1}{U_h D_h(0)}\right)\left(1-\frac{T}{T_C}\right)^{\frac{1}{2}}. \quad (36)$$

Where the experimental value of the density of states and the pairing potentials [23] are the density of states at the Fermi level and the pairing interaction potential for a hole intra-band transition, respectively.

The inter-band transition between the electron and hole bands, the superconducting order parameter can be related to the Green's function as

$$\Delta_{eh} = \frac{U_{eh}}{4\beta}\sum_k(\langle\langle \hat{C}^+_{k\uparrow}, \hat{C}^+_{-k\downarrow}\rangle\rangle + \langle\langle \hat{d}^+_{k\uparrow}, \hat{d}^+_{-k\downarrow}\rangle\rangle). \quad (37)$$

Performing the same procedures as for the electron intra-band transitions computed above, the expression for the superconducting order parameter in the inter-band transitions $\Delta_{eh}(T)$ reads

$$\Delta_{eh}(T) = 3.49\,\hbar\omega_{\rm F}\times$$
$$\times\exp\left(-\frac{1}{U_{eh}\sqrt{D_e(0)D_h(0)}}\right)\left(1-\frac{T}{T_C}\right)^{\frac{1}{2}}. \quad (38)$$

2.2. Dependence of the superconducting transition temperature on the inter-band pairing potential

By coupling the two superconducting equations given below, the dependence of the superconducting transition temperature on the inter-band interaction potential can be expressed as follows [23]:

$$\Delta_e = U_e(0)D_e(0)\int_0^{\hbar\omega_{\rm F}}\frac{\tanh\left(\frac{\beta(E_e(k))}{2}\right)}{E_e(k)}dE_e(k) +$$
$$+ U_{eh}D_h(0)\Delta_h\int_0^{\hbar\omega_{\rm F}}\frac{\tanh\left(\beta\frac{E_h(k)}{2}\right)}{E_h(k)}dE_h(k) \quad (39)$$

and

$$\Delta_h = U_h(0)D_h(0)\int_0^{\hbar\omega_{\rm F}}\frac{\tanh\left(\frac{\beta(E_h(k))}{2}\right)}{E_h(k)}dE_h(k) +$$
$$+ U_{eh}D_e(0)\Delta e\int_0^{\hbar\omega_{\rm F}}\frac{\tanh\left(\beta\frac{E_e(k)}{2}\right)}{E_e(k)}dE_e(k). \quad (40)$$

Now, let

$$\int_0^{\hbar\omega_{\rm F}}\frac{\tanh\left(\beta\frac{E_e(k)}{2}\right)}{E_e(k)}dE_e(k) = f(A)$$

and

$$\int_0^{\hbar\omega_{\rm F}} \frac{\tanh\left(\beta\frac{E_h(k)}{2}\right)}{E_h(k)}\, dE_h(k) = f(A). \quad (41)$$

Using (41) in (39) and (40), we get

$$\Delta_e = U_e D_e(0)\Delta_e f(A) + U_{eh} D_h(0)\Delta_h f(B), \quad (42)$$

and

$$\Delta_h = U_h D_h(0)\Delta_h f(A) + U_{eh} D_e(0)\Delta_e f(B). \quad (43)$$

Rearranging (42) and (43), we get, respectively,

$$\Delta_e \left[1 - U_e D_e(0) f(A)\right] = U_{eh} D_h(0)\Delta_h f(B), \quad (44)$$

and

$$\Delta_h \left[1 - U_h D_h(0) f(A)\right] = U_{eh} D_e(0)\Delta_e f(B). \quad (45)$$

Considering the product of (44) and (45), we obtain

$$\left[1 - U_e D_e(0) f(A)\right]\left[1 - U_h D_h(0) f(B)\right] =$$
$$= U_{eh}^2 D_h(0) f(B) D_e(0) f(A). \quad (46)$$

At $T = T_C, \Delta_e = \Delta_h = 0$. Thus, we have $f(A) = f(B) = f(T_C)$.

Hence, (46) becomes

$$\left[U_{eh}^2 - U_e U_h\right] f^2(T_C) +$$
$$+ \left[\frac{U_e}{D_h(0)} + \frac{U_h}{D_e(0)}\right] f(T_C) - \frac{1}{D_e(0) D_h(0)} = 0. \quad (47)$$

Therefore, the solution of (47) is given by

$$f(T_C) = \left(\frac{1}{2}\left(\frac{U_e}{D_h(0)} + \frac{U_h}{D_e(0)}\right) - \right.$$
$$\left. - \sqrt{\frac{1}{4}\left(\frac{U_e}{D_h(0)} + \frac{U_h}{D_e(0)}\right)^2 + \left(\frac{U_{eh}^2 - U_e U_h}{D_e(0) D_h(0)}\right)}\right) /$$
$$(U_{eh}^2 - U_e U_h). \quad (48)$$

But, at

$$T = T_C, f(T_C) = \ln(1.14\frac{\hbar\omega_{\rm F}}{k_{\rm B} T_C}.$$

Hence, (48) becomes

$$\ln 1.14\frac{\hbar\omega_{\rm F}}{k_{\rm B} T_C} = \left(-\frac{1}{2}\left(\frac{U_e}{D_h(0)} + \frac{U_h}{D_e(0)}\right) - \right.$$
$$\left. - \sqrt{\frac{1}{4}\left(\frac{U_e}{D_h(0)} + \frac{U_h}{D_e(0)}\right)^2 + \left(\frac{U_{eh}^2 - U_e U_h}{D_e(0) D_h(0)}\right)}\right) /$$
$$(U_{eh}^2 - U_e U_h).$$

Finally, the dependence of the superconducting transition temperature on the intra-band s and inter-band interaction potentials is given by

$$T_C = 1.14\,\frac{\hbar\omega_{\rm F}}{k_{\rm B}} \exp\Big(\big(-U_e D_e(0) - U_h D_h(0) -$$
$$- \sqrt{(U_e D_e(0) + U_h D_h(0))^2 + 4(U_{eh}^2 - U_e U_h) D_e(0) D_h(0)}\big) /$$
$$\left(2(U_{eh}^2 - U_e U_h) D_e(0) D_h(0)\right)\Big). \quad (49)$$

Now, if the intra-band interaction potentials are ignored, and the superconducting transition temperature is induced only by the inter-band interaction potential, (49) reduces to

$$T_C = 1.14\,\frac{\hbar\omega_{\rm F}}{k_{\rm B}} \exp\left(-\frac{1}{U_{eh}\sqrt{D_e(0) D_h(0)}}\right). \quad (50)$$

Thus, (50) yields the dependence of the superconducting transition temperature ($T_{\rm C}$) on the inter-band interaction potential in the two-band model mediated by the inter-band pairing interaction. Therefore, one can easily observe that, by taking the electron intra-band pairing potential and the hole intra-band pairing potential equal to zero, the inter-band interaction potential can induce the superconducting transition temperature $T_{\rm C}$.

2.3. Electronic specific heat in the electron and hole ntra-bands

The electronic specific heat per atom of a superconducting material for the electron intra-bands is determined using the following relation [24, 25]:

$$C_{es}^e = \frac{\partial}{\partial T}\frac{1}{D_e(T)}\sum_p \varepsilon_e(k)\langle\langle \hat{C}_{k\uparrow}^+, \hat{C}_{k\uparrow}, \rangle\rangle, \quad (51)$$

where $\varepsilon_e(k)$ is the electron energy and $D_e(T)$ is the density of states.

By employing the Green‘ function given by $\langle\langle \hat{C}_{k\uparrow}^+, \hat{C}_{k\uparrow}, \rangle\rangle$ changing the summation into the integration, and using the relation $\sum_k = D_e(0)\int d\varepsilon_e(k)$,

we obtain

$$\hat{C}^e_{es} = \frac{2D_e(0)}{N}\int\limits_0^{\hbar\omega_{\rm F}} d\varepsilon_e(k)\left(\left(\frac{\beta\varepsilon_e(k)\alpha_2\exp(\beta\alpha_2)}{T\left(\exp(\beta\alpha_2)+1\right)^2}\right)+\right.$$

$$\left.+\frac{\beta(\alpha_1-\varepsilon_e(k)\varepsilon_e(k)}{2T\sqrt{\varepsilon_e^2(k)+\Delta_e^2+\Delta_{eh}^2+\Delta_e\Delta_{eh}+\Delta_{eh}\Delta_e}}\right)\times$$

$$\times\left[\frac{\alpha_1\exp(\beta\alpha_1)}{\left[\exp(\beta\alpha_1\right]^2}-\left[\frac{\alpha_2\exp(\beta\alpha_2)}{\left[\exp(\beta\alpha_1)-1\right]^2}\right]\right], \quad (52)$$

where

$$\alpha_1 = +\sqrt{\varepsilon_e^2(k)+(\Delta_e+\Delta_{eh})^2}.$$

Since each intra-band can be treated separately, the inter-band interaction can be ignored [26]. Thus, under this assumption, we get

$$\alpha_1 = \sqrt{\varepsilon_e^2(k)+\Delta_e^2}.$$

and

$$\alpha_2 = -\sqrt{\varepsilon_e^2(k)+(\Delta_e+\Delta_{eh})^2}.$$

Similarly, in the absence of the inter-band interaction $\Delta_{eh}=0$ [26], we have

$$\alpha_2 = -\sqrt{\varepsilon_e^2(k)+\Delta_e^2}.$$

Now, substituting the values of alpha one and α_1 and alpha two $\alpha_2$into (52) and performing a couple of steps, we get

$$\frac{C^e_{es}}{T} = \frac{2}{D_e(0)k_{\rm B}T^2}\times$$

$$\times\int\limits_0^{\hbar}\varepsilon_e^2(k)\,d\varepsilon_e(k)\sec h^2\left(\frac{\sqrt{\varepsilon_e^2(k)+\Delta_e^2}}{2k_{\rm B}T}\right). \quad (53)$$

Furthermore, by applying a similar procedure as for the electronic specific heat for the electron intra-band above, we obtain the expression for the electronic specific heat for the hole intra-band to be

$$\frac{C^h_{es}}{T} = \frac{2}{D_e(0)k_{\rm B}T^2}\times$$

$$\times\int\limits_0^{\hbar}\varepsilon_e^2(k)d\varepsilon_e(k)\sec h^2\left(\frac{\sqrt{\varepsilon_e^2(k)+\Delta_e^2}}{2k_{\rm B}T}\right). \quad (54)$$

2.4. Entropy in the electron and hole intra-bands

As is well known, the entropy is a measure of disorder of a system [27]. From the thermodynamic relations, the entropy is evaluated from the electron specific heat [28]. So, the entropy for the electron intra-band is expressed as

$$S_e = \int\limits_0^T C^e_{es}\frac{dT}{T}. \quad (55)$$

Now, using (53) in (55), we get

$$S_e = \int\limits_0^T \frac{2}{D_e(0)k_{\rm B}T}\times$$

$$\times\int\limits_0^{\hbar\omega_{\rm F}}\varepsilon_e^2(k)d\varepsilon_e(k)\sec h^2\left(\frac{\sqrt{\varepsilon_e^2(k)+\Delta_e^2}}{2k_{\rm B}T}\right)\frac{dT}{T}. \quad (56)$$

Thus, we obtain the entropy of the electron intra-band to be

$$S_e = \frac{2}{D_e(0)k_{\rm B}}\times$$

$$\times\int\limits_0^T\int\limits_0^{\hbar\omega_{\rm F}}\frac{1}{\rm T}\,\varepsilon_e^2 d\varepsilon_e(k)dT\sec h^2\left(\frac{\sqrt{\varepsilon_e^2(k)+\Delta_e^2}}{2k_{\rm B}}\right). \quad (57)$$

Furthermore, by using (54) and applying a similar procedure as for the entropy for the electron intra-band above, we obtain the expression for the entropy for the hole intra-band to be

$$S_h = \frac{2}{D_h(0)k_{\rm B}}\times$$

$$\times\int\limits_0^T\int\limits_0^{\hbar\omega_{\rm F}}\frac{1}{T}\varepsilon_h^2 d\varepsilon_h(k)\,dT\sec h^2\left(\frac{\sqrt{\varepsilon_h^2(k)+\Delta_h^2}}{2k_{\rm B}}\right). \quad (58)$$

2.5. Density of states in the electron and hole intra-bands

The dependence of the density of states on the excitation energy εin the electron band [29, 30] is given by

$$D_e(\varepsilon) = \lim_{\varepsilon_e\to 0}\frac{1}{2\pi}\sum_k\Big[G_{\uparrow\uparrow}(k,\varepsilon+i\varepsilon_e(k))-$$

$$-G_{\downarrow\downarrow}(k,\varepsilon-i\varepsilon_e(k))\Big], \quad (59)$$

where the density of states is dependent on the Green function $G_{\uparrow\uparrow}$ for the electron band.

Now, using (14) in (19), we have

$$\langle\langle \hat{C}_{-k\downarrow}, \hat{C}^{+}_{-k\downarrow}\rangle\rangle = \frac{\varepsilon + \varepsilon_e(k)}{\varepsilon^2(k) - E_e^2(k)}, \tag{60}$$

where $E_e^2(k) = \varepsilon_e^2(k) + \Delta_e^2$.

By using the partial fraction method, (60) becomes

$$\langle\langle \hat{C}_{-k\downarrow}, \hat{C}^{+}_{-k\downarrow}\rangle\rangle = \frac{1}{2}\left(\frac{1}{\varepsilon(k) - E_e(k)}\right)\left(1 + \frac{\varepsilon_e(k)}{E_e(k)}\right) + \\ + \frac{1}{2}\left(\frac{1}{\varepsilon + E_e(k)}\right)\left(1 - \frac{\varepsilon_e(k)}{E_e(k)}\right). \tag{61}$$

Using the definition of the Dirac delta function, the expression for the density of states for the electron intra-band given in (59) becomes

$$D_e(\varepsilon) = \frac{1}{2}\sum_k \left[\left(1 + \frac{\varepsilon_e(k)}{E_e(k)}\right)\delta(\varepsilon(k) - E_e(k)) + \right. \\ \left. + \left(1 - \frac{\varepsilon_e(k)}{E_e(k)}\right)\delta(\varepsilon(k) + E_e(k))\right]. \tag{62}$$

Now, changing the summation into the integration in (62) and assuming the density of states does not make any variation over this integral, we get

$$D_e(\varepsilon) = D_e(0)\int_0^{\hbar\omega_{\rm F}}\left(1 + \frac{\varepsilon_e(k)}{E_e(k)}\right)\delta(\varepsilon(k) - E_e(k))d\varepsilon_e(k) + \\ + D_e(0)\int_0^{\hbar\omega_{\rm F}}\left(1 - \frac{\varepsilon_e(k)}{E_e(k)}\right)\delta(k) + E_e(k) + E_e(k))d\varepsilon_e(k). \tag{63}$$

Applying the Dirac delta integration properties such that $\int f(x)\delta(x-a))dx = f(a)$, we obtain

$$D_e(\varepsilon) = D_e(0)\left(\frac{2\varepsilon_e(k)}{E_e(k)}\right). \tag{64}$$

Finally, for $\varepsilon_e(k) = \varepsilon(k)$ and $E_e^2(k) = \varepsilon_e^2(k) + \Delta_e^2$, we get

$$D_e(\varepsilon) = \begin{cases} 2D_e(0)\dfrac{\varepsilon(k)}{\varepsilon^2(k) - \Delta_e^2} & \text{for } \varepsilon(k) \geqslant \Delta_e, \\ 0 & \text{for } \varepsilon(k) < \Delta_e. \end{cases} \tag{65}$$

Similarly, applying the same procedure as for the electron intra-band above, the density of states in the hole intra-band becomes

$$D_h(\varepsilon) = \begin{cases} 2D_h(0)\dfrac{\varepsilon(k)}{\varepsilon^2(k) - \Delta_h^2} & \text{for } \varepsilon(k) \geqslant \Delta_h, \\ 0 & \text{for } \varepsilon(k) < \Delta_h. \end{cases} \tag{66}$$

2.6. Condensation energy in the iron-based superconductor $Ba_{1-x}Na_xFe_2As_2$

The comprehension of the origin of the condensation energy E_C is a vital step toward identifying the mechanism of high-temperature superconductivity [31, 32]. The value of the condensation energy E_C is a measure of how much stable the superconducting state is as compared to the normal state. The condensation energy in the two-band model is given by [33]

$$E_C = \langle E_S\rangle - \langle E_N\rangle, \\ E_C = (E_{\rm kin(s)} - E_{\rm kin(n)}) + (E_{\rm po(S)} - E_{\rm po(n)}), \\ E_C = \Delta KE + \Delta PE. \tag{67}$$

The change in the kinetic energy in (67) is given as

$$\Delta KE = -\frac{1}{2}D_e(0)\Delta_e^2 - \frac{1}{2}D_h(0)\Delta_h^2. \tag{68}$$

Similarly, the change in the potential energy in (67) is given as

$$\Delta PE = \frac{\Delta_h^*\Delta_e}{U_{eh}} + \frac{\Delta_e^*\Delta_h}{U_{eh}}.$$

Since the superconducting order parameters in each band are real, $\Delta^*_{e(h)} = \Delta_{e(h)}$. Thus, we obtain

$$\Delta PE = 2\frac{\Delta_h\Delta_e}{U_{eh}}. \tag{69}$$

For the inter-band pairing potential less than $U_{eh} < 0$ (attractive), the intra-band order parameters have the same sign. Hence, (67) becomes

$$E_C = -\frac{1}{2}D_e(0)\Delta_e^2 - \frac{1}{2}D_h(0)\Delta_h^2 + \\ + 2\frac{\Delta_h\Delta_e}{U_{eh}} + 2\frac{\Delta_h\Delta_e}{U_{eh}}. \tag{70}$$

Substituting (33) and (36) into (70) for Δ_e^2 and, respectively using the values of the different parameters, we get the expression for the condensation energy to be

$$E_C = \left(-0.48 + \frac{52.178}{U_{eh}}\right) \times 10^3\left(1 - \frac{T}{T_C}\right). \tag{71}$$

3. Results and Discussion

In this work, we have used the model Hamiltonian developed for the two-band iron-based superconductor IBSC $Ba_{1-x}Na_xFe_2As_2$. We obtained the expressions for the temperature dependence of the superconducting order parameters for the intra-band, inter-band, and electronic specific heat. Moreover, we obtained the dependences of the superconducting transition temperature (T_C) on the inter-band pairing potential U_{eh}, density of states $D(E)$on the excitation energy, and the condensation energy E_C on the temperature, pairing interaction potential, and superconducting transition temperature.

Now, by using (33), (36), and (38) and some experimental values for the two-band model high-temperature IBSC $Ba_{1-x}Na_xFe_2As_2$ and applying some credible approximations, we plotted the phase diagram of electron intra-band $\Delta_e(T)$, hole intra-band $\Delta_h(T)$, inter-band $\Delta_{eh}(T)$, and the total superconducting order parameter versus the temperature as shown in Fig. 1.

As can be seen from Fig. 1, as the temperature increases, all the superconducting order parameters decrease and vanish at the transition temperature (T_C) of $Ba_{1-x}Na_xFe_2As_2$. From Fig. 1, we have compared physically the theoretical results with experimental data and have a significant difference at zero temperature. All are decrease with increasing the temperature, and all vanish at the critical temperature.

Secondly, using (50), we have shown a variation of the superconducting transition temperature with the inter-band interaction potential of $Ba_{1-x}Na_xFe_2As_2$ as shown in Fig. 2.

One can observe from Fig. 2 that, as the interaction inter-band pairing potential U_{eh} increases, the superconducting temperature increases and vice versa for the substance under consideration. From Fig. 2, we have compared physically the theoretical results with experimental findings: all are originated at the same point, and all increase with increasing the inter-band pairing potential.

Thirdly, by considering (53) and (54), we plotted the phase diagram for the electronic specific heat in the electron intra-band, $C^e_{es}(T)$, and the specific heat for the hole intra-band, $C^h_{es}(T)$, versus the temperature, as depicted in Fig. 3.

As can be seen from Fig. 3, the electronic specific heat for both electron and hole intra-bands

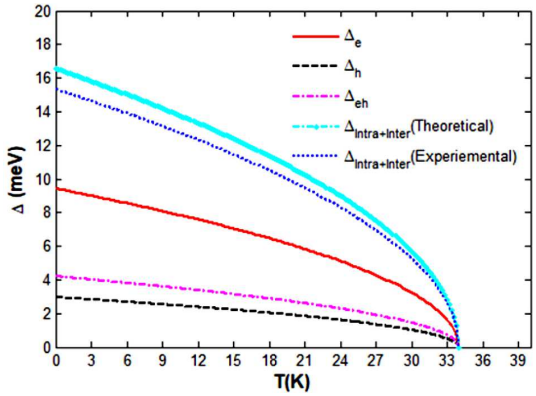

Fig. 1. Superconducting order parameters versus the temperature for the iron-based superconductor $Ba_{1-x}Na_xFe_2As_2$

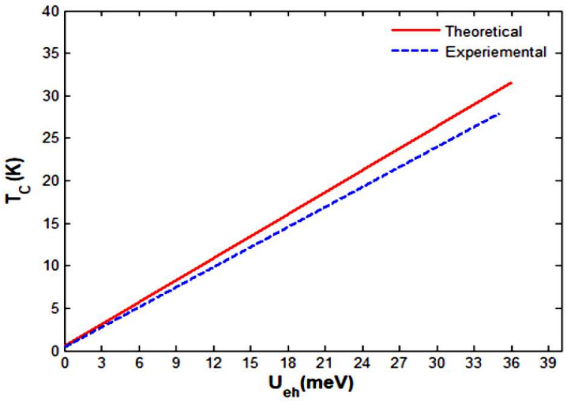

Fig. 2. Superconducting transition temperature versus the inter-band pairing potential energy for the iron-based superconductor $Ba_{1-x}Na_xFe_2As_2$

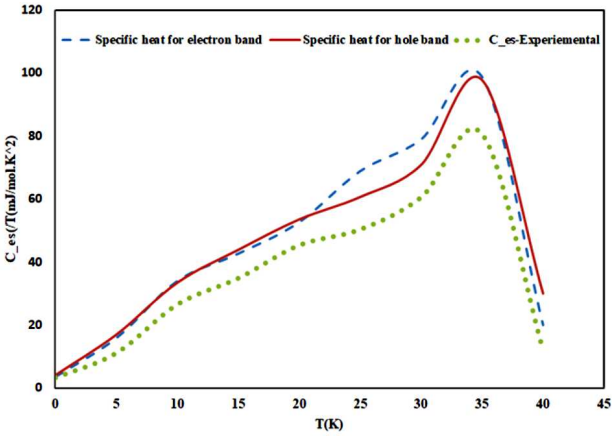

Fig. 3. Electronic specific heat versus the temperature for iron-based superconductor $Ba_{1-x}Na_xFe_2As_2$

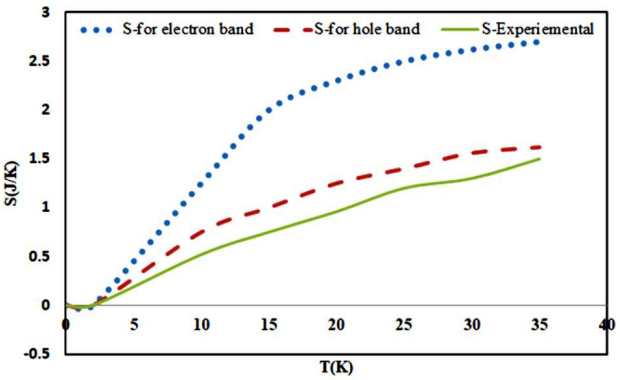

Fig. 4. Entropy (S) versus the temperature for IBSC $Ba_{1-x}Na_xFe_2As_2$

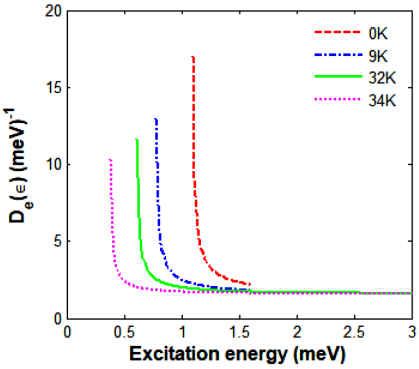

Fig. 5. Density of states for the electron intra-band at different temperature values versus the excitation energy for the iron-based superconductor

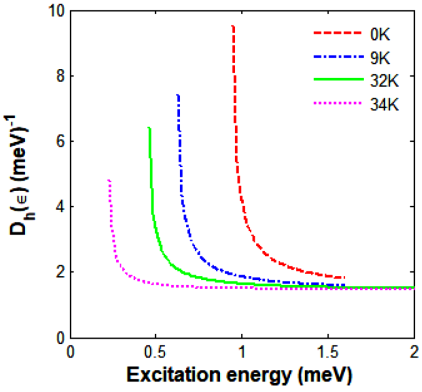

Fig. 6. Density of states for the hole intra-band at different temperature values versus the excitation energy for iron-based superconductor $Ba_{1-x}Na_xFe_2As_2$

increases with the temperature and sharply decreases at the transition temperature $T_C = 34$ K of $Ba_{1-x}Na_xFe_2As_2$. This is due to the fact that, when

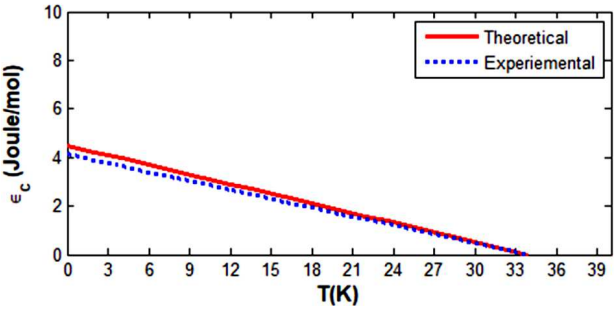

Fig. 7. Condensation energy versus the temperature for iron-based superconductor $Ba_{1-x}Na_xFe_2As_2$

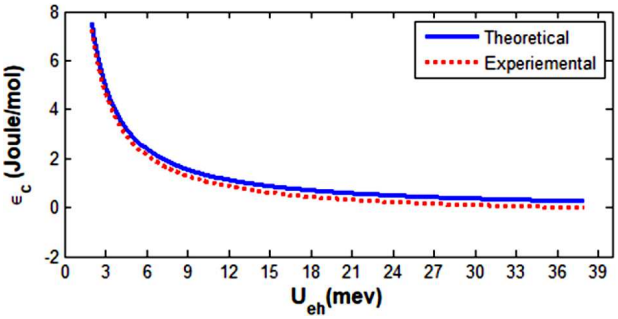

Fig. 8. Condensation energy versus the inter-band pairing potential at $T = 0$ K for iron-based superconductor $Ba_{1-x}Na_xFe_2As_2$

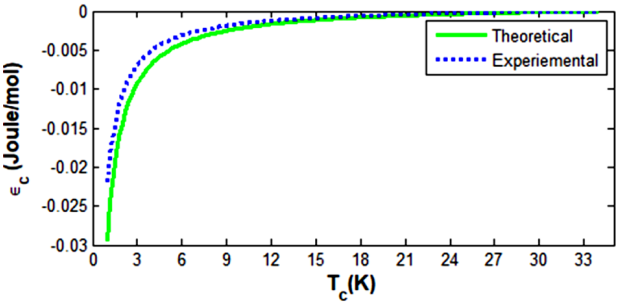

Fig. 9. Condensation energy versus the superconducting transition temperature for iron-based superconductor $Ba_{1-x}Na_xFe_2As_2$

the material becomes superconducting at zero magnetic field, its electronic specific heat jumps at the transition temperature (T_C) and then decays, since the transition is continuous, as the latent heat is not released during the process. From Fig. 3, we have also compared the theoretical and experimental data. All are originated from the same point, and all increase with the temperature up to the critical temperature and decrease after the critical temperature.

By considering (57) and (58), we have plotted the phase diagrams for the entropy in the electron intra-band $S_e(T)$ and in the hole intra-band $S_h(T)$ versus the temperature as depicted in Fig. 4.

As can be seen from Fig. 4, the entropy for both electron and hole intra-bands increase with the temperature up to the transition temperature ($T_{\rm C} = 34$ K) of $Ba_{1-x}Na_xFe_2As_2$. Furthermore, by considering (65) and (66), we plotted the phase diagrams for the density of states in the electron intra-band $D_e(E)$ and density of states in the hole intra-band $D_h(E)$ versus the excitation energy for different values of the temperature as shown in Figs. 5 and 6, respectively. From Fig. 4, we have compared the theoretical and experimental findings. All are originated from the same point, and all increase with the temperature up to the critical temperature.

From Figs. 5 and 6, one can observe that the variation of the densities of states of both the electron and hole intra-bands with the excitation energy is analogous. Furthermore, it can be seen from the figures that both densities of states decrease as the value of the temperature increases.

Finally, using (71), we plotted the phase diagrams of the condensation energy versus the temperature, condensation energy versus the inter-band pairing potential U_{eh} at $T = 0$ K, and condensation energy versus the superconducting transition temperature as shown in Figs. 7–9, respectively, for the IBSC $Ba_{1-x}Na_xFe_2As_2$.

As can be seen from Fig. 7, the condensation energy decreases as the temperature increases and vanishes at the transition temperature. In Fig. 8, the condensation energy decreases, as the inter-band pairing potential increases. Lastly in Fig. 9, the condensation energy increases, as the temperature increases, and tends to be constant at the condensation energy equal to zero, $E_C = 0$. In Figs. 7–9 respectively, we have compared the theoretical and experimental findings that reveal a significant difference.

4. Conclusion

In this research work, we have studied the two-band model high-temperature IBSC $Ba_{1-x}Na_xFe_2As_2$ by developing a model Hamiltonian and by using the well-known double-time temperature-dependent Green's function technique. The superconducting order parameters for electron intra-band $\Delta_e(T)$, hole intra-band $\Delta_h(T)$ and inter-band $\Delta_{eh}(T)$ versus the temperature phase diagrams are demonstrated in Fig. 1 and have different values at zero temperature, decrease as the temperature increases, and all vanish at the superconducting transition temperature ($T_{\rm C}$) due to the presence of the inter-band hopping in $Ba_{1-x}Na_xFe_2As_2$. Furthermore, as demonstrated in Fig. 2, the superconducting transition temperature increases, as the inter-band pairing potential U_{eh} increases. The occurrence of the inter-band transitions enriches the pairing of electrons and forces the system to have a single superconducting transition temperature. In Fig. 3, we have shown the variation of the electronic specific heat for both the electron and hole intra-bands. One can easily observe the increase of the electronic specific heat, as the temperature increases, and the abrupt decrease in the electronic specific heat of both bands at the transition temperature. The increase of the entropy of both bands with the temperature is also demonstrated in Fig. 4. Likewise, in Figs. 5 and 6, the density of states for the electron and hole intra-bands vary in a similar manner with the excitation energy and decrease as the value of the temperature is increased. Lastly, in Figs. 7–9, we have portrayed the dependence of the condensation energy on the temperature, on the inter-band pairing potential, and on the superconducting transition temperature, respectively. The figures show that, with increasing the temperature, the inter-band pairing potential, superconducting transition temperature, and the magnitude of the condensation energy decrease. The results we obtained in the current research work are in a broad agreement with previous findings [29, 34, 35].

5. Conflict of Interest

There is no self-interested thinking on the part of any of the authors of this study with regard to this publication, the research results that have been published, the costs associated with doing the research, acquiring and using its results, or any non-financial personal relationships.

1. H. Hosono, A. Yamamoto, H. Hiramatsu, Y. Ma. Recent advances in iron-based superconductors toward applications. *Materials Today* **21** (3), 278 (2018).
2. Y. Kamihara, T. Watanabe, M. Hirano, H. Hosono. Iron-Based Layered Superconductor $La[O_{1-x}F_x]FeAs$ ($x = 0.05$–0.12) with $T_{\rm C} = 26$ K. *J. Am. Chem. Soc,* **130** (11), 3296 (2008).

3. H. Takahashi, K. Igawa, K. Arii, Y. Kamihara, M. Hirano, H. Hosono. Superconductivity at 43 K in an iron-based layered compound $LaO_{1-x}F_xFeAs$. *Nature* **453** (7193), 376 (2008).
4. M. Rotter, M. Tegel, D. Johrendt. Superconductivity at 38 K in the iron arsenide $(Ba_{1-x}K_x)Fe_2$ As_2. *Phys. Rev. Lett.* **101** (10), 107006 (2008).
5. H. Huang, C. Yao, C. Dong, X. Zhang, D. Wang, Z. Cheng, J. Li, S. Awaji, H. Wen, Y. Ma. High transport current superconductivity in powder-in-tube $Ba_{0.6}K_{0.4}Fe_2As_2$ tapes at 27 T. *Supercond. Sci. Technol.* **31**(1), 015017 (2017).
6. V. Stanev, J. Kang, Z. Tesanovic. Spin fluctuation dynamics and multiband superconductivity in iron pnictides. *Phys. Rev. B* **78** (18), 184509 (2008).
7. M. Ishikado, S. Shamoto, K. Kodama, R. Kajimoto, M. Nakamura, T. Hong, H. Mutka. High-energy spin fluctuation in low-Tc iron-based superconductor $LaFePO_{0.9}$. *Sci. Rep.* **8** (1), 1 (2018).
8. J. Hecher, T. Baumgartner, J.D. Weiss, C. Tarantini, A. Yamamoto, J. Jiang, E.E. Hellstrom, D.C. Larbalestier, M. Eisterer. Small grains: a key to high-field applications of granular Ba-122 superconductors? *Supercond. Sci. Technol.* **29** (2), 025004 (2016).
9. S. Aswartham, M. Abdel-Hafiez, D. Bombor, M. Kumar, A.U.B. Wolter, C. Hess, D.V. Evtushinsky, V.B. Zabolotnyy, A.A. Kordyuk, T.K. Kim, S.V. Borisenko, G. Behr, B. Büchner, S. Wurmehl. Hole doping in $BaFe_2As_2$: The case of $Ba_{1-x}Na_x$ Fe_2As_2 single crystals. *Phys. Rev. B* **85** (22), 224520 (2012).
10. D.V. Evtushinsky, V.B. Zabolotnyy, L. Harnagea, A.N. Yaresko, S. Thirupathaiah, A.A. Kordyuk, J. Maletz, S. Aswartham, S. Wurmehl, E. Rienks, R. Follath, B. Büchner, S.V. Borisenko. Electronic band structure and momentum dependence of the superconducting gap in $Ca_{1-x}Na_xFe_2As_2$ from angle-resolved photoemission spectroscopy. *Phys. Rev. B* **87** (9), 094501 (2013).
11. A.A. Kordyuk. Iron-based superconductors: Magnetism, superconductivity, and electronic structure. *Low Temperature Physics* **38** (9), 888 (2012).
12. O.L.T. de Menezes. Importance of hybrid pairs in superconductors. *Solid State Commun.* **57** (10), 825 (1986).
13. Y. Zhang, L.X. Yang, M. Xu, Z.R. Ye, F. Chen, C. He, H.C. Xu, J. Jiang, B.P. Xie, J.J. Ying, X.F. Wang, X.H. Chen, J.P. Hu, M. Matsunami, S. Kimura, D.L. Feng. Nodeless superconducting gap in $A_xFe_2Se_2$ (A = K, Cs) revealed by angle-resolved photoemission spectroscopy. *Nature Mat.* **10** (4), 273 (2011).
14. D.J. Singh. Electronic structure and doping in $BaFe_2As_2$ and LiFeAs: Density functional calculations. *Phys. Rev. B* **78** (9), 094511 (2008).
15. T. Kidanemariam, G. Kahsay. Theoretical study of superconducting gap parameters, density of states, and condensation energy of two-band iron-based superconductor $BaFe_2(As_{1-x}P_x)_2$. *J. Supercond. Nov. Magn.* **31** (1), 37 (2018).
16. E. Sheveleva, B. Xu, P. Marsik, F. Lyzwa, B.P.P. Mallett, K. Willa, C. Meingast, Th. Wolf, T. Shevtsova, Yu.G. Pashkevich, C. Bernhard. Muon spin rotation and infrared spectroscopy study of $Ba_{1-x}Na_xFe_2As_2$. *Phys. Rev. B* **101** (22), 224515 (2020).
17. H. Suhl, B.T. Matthias, L.R. Walke. Bardeen–Cooper–Schrieffer theory of superconductivity in the case of overlapping bands. *Phys. Rev. Lett.* **3** (12), 552 (1959).
18. B.K. Chakraverty. Superconductive solutions for a two-band Hamiltonian. *Phys. Rev. B* **48** (6), 4047 (1993).
19. T. Chanpoom, J. Seechumsang, S. Chantrapakajee, P. Udomsamuthirun. The study on hybridized two-band superconductor. *Advan. Cond. Matter Phys.* **2013** (2013).
20. D.N. Zubarev. Double-time Green functions in statistical physics. *Sovt. Phys. Usp.* **3** (3), 320 (1960).
21. N. Agustin. Evaluating sums over the Matsubara frequencies. *Computer Phys. Commun.* **92** (1), 54 (1995).
22. J. Bardeen, L.N. Cooper, J.R. Schrieffer. Theory of superconductivity. *Phys. Rev.* **108** (5), 1175 (1957).
23. B. Yunkyu, G.R. Stewart. Anomalous scaling of ΔC versus T_C in the Fe-based superconductors: the $S_{\pm}$-wave pairing state model. *New J. Phys.* **18** (2), 023017 (2016).
24. I.I. Mazin, V.P. Antropo. Electronic structure, electron–phonon coupling, and multiband effects in MgB_2, *Physica C* **385** (1–2), 49 (2003).
25. N. Kristoffel, P. Rubin. Pseudogap and superconductivity gaps in a two-band model with doping-determined components. *Solid State Commun.* **122** (5), 265 (2002).
26. H. Padamsee, J.E Neighbor, C.A. Shiffman. Quasiparticle phenomenology for thermodynamics of strong-coupling superconductors. *J. Low Temp. Phys.* **12** (3), 387 (1973).
27. J.O. Odhiambo, Y.K. Ayodo, T.W. Sakwa, B.W. Rapando. Thermodynamic properties of Mercury based cuprate due to Cooper pair – electron interaction. *JMEST* **3** (7), 5241 (2016).
28. O.O. Jared, M.J. Wanjala. Specific heat and entropy of a three electron model in bismuth based cuprate superconductor. *World J. App. Phys.* **3** (2), 19 (2018).
29. A. Nuwal, S. Kakani, S. Lal Kakani. Generalized multiple gap model for the superconductivity in Fe–As based superconductors. *SOP Trans. Theor. Phys.* **1** (2), 7 (2014).
30. A.K. Pramanik, M. Abdel-Hafiez, S. Aswartham, A.U.B. Wolter, S. Wurmehl, V. Kataev, B. Büchner. Multigap superconductivity in single crystals of $Ba_{0.65}Na_{0.35}Fe_2As_2$: A calorimetric investigation. *Phys. Rev. B* **84** (6), 064525 (2011).
31. S.P. Kruchinin, H. Kawabe, H. Nagao, Y. Nakazawa. Condensation energy for a two-gap superconducting state in nanoparticles. *J. Nanoparticles* **2013**, 1 (2013).
32. R. Haslinger, A.V. Chubukov. Condensation energy in strongly coupled superconductors. *Phys. Rev. B* **67** (21), 140504 (2003).
33. B. Yunkyu. The origin of the condensation energy scaling of iron-based superconductors. *EPL* **115** (2), 27002 (2016).
34. A. Nuwal, S. Lal Kakani. Theoretical study of specific heat and density of states of MgB_2 superconductor in two

band model. *World J. Condens. Matter Phys.* **3** (2), 1 (2013).

35. P. Popovich, A.V. Boris, O.V. Dolgov, A.A. Golubov D.L. Sun, C.T. Lin, R.K. Kremer, B. Keimer. Specific heat measurements of $Ba_{0.68}K_{0.32}Fe_2As_2$ single crystals: Evidence for a multiband strong-coupling superconducting state. *Phys. Rev. Lett.* **105** (2), 027003 (2010).

Received 31.12.21

Т. Ліссану, Г. Касей, Т. Негуссі

ТЕОРЕТИЧНЕ ДОСЛІДЖЕННЯ
В РАМКАХ ДВОЗОННОЇ МОДЕЛІ НАДПРОВІДНИХ
ТА ТЕРМОДИНАМІЧНИХ ВЛАСТИВОСТЕЙ
ВИСОКОТЕМПЕРАТУРНОГО НАДПРОВІДНИКА
НА ОСНОВІ ЗАЛІЗА $Ba_{1-x}Na_xFe_2As_2$

Виконано теоретичне дослідження надпровідникових та термодинамічних властивостей високотемпературного надпровідника на основі заліза $Ba_{1-x}Na_xFe_2As_2$ в рамках двозонної моделі. Побудовано модельний гамільтоніан із використанням двочасової температурозалежної функції Гріна, розраховано параметри порядку для переходів електрона та дірки в зоні та між зонами, температуру переходу в надпровідний стан, густини станів та енергії конденсації. Розраховано питому теплоту та ентропію для переходів електронів і дірок у зоні. Використовуючи експериментальні дані та деякі наближення, ми побудували фазові діаграми для параметрів порядка як функцій температури, розрахували залежність критичної температури від потенціалу міжзонної взаємодії, температурні залежності питомої теплоти і ентропії для переходів електронів і дірок у зоні та залежність густини станів для таких переходів від енергії збудження для різних значень температури. Крім того, знайдено залежності енергії конденсації від температури, міжзонного потенціалу двійкування при $T = 0$ K від енергії конденсації та енергії конденсації від температури T_C переходу в надпровідний стан. Виконано порівняння теоретичних і експериментальних значень. Отримані результати добре узгоджуються з попередніми.

Ключові слова: параметри порядка, питома теплота, густина станів, енергія конденсації, $Ba_{1-x}Na_xFe_2As_2$.